Seismic Performance Assessment of Corroded Reinforced Concrete Columns Based on Codal Provision and Empirical Formulations

Rubeen Kumar[1], Harish Chandra Arora[2,3], Aman Kumar[2,3*], Prashant Kumar[2,3,5], Surabhi Sharma[1], Madhu Sharma[4]

[1] Department of Civil Engineering, Jawaharlal Nehru Government Engineering College, 175018 Sundernagar, India
[2] Structural Engineering Division, CSIR-Central Building Research Institute, 247667 Roorkee, India
[3] Academy of Scientific and Innovative Research (AcSIR), 201002 Ghaziabad, India
[4] Department of Civil Engineering, Government Hydro Engineering College, 174001 Bilaspur, India
[5] Civil Engineering Department, COER University, 247667, Roorkee, India
* Corresponding author, e-mail: aman.civil17@gmail.com

Abstract

Corrosion is a major threat to the early degradation of reinforced concrete (RC) structures. This deterioration leads to a reduction in the overall ductility and load-carrying capacity of RC structures. In RC structures, columns play a crucial role as columns take both structural and seismic loads. When columns are affected by corrosion and subjected to seismic events simultaneously, columns may collapse suddenly. This sudden failure poses risks to human beings as well as the surrounding environment. Hence, evaluating the residual capacity of corroded RC columns is essential to implement preventive and rehabilitation measures before a catastrophic failure occurs. The objective of the current study was to assess the performance and reliability of existing design guidelines and analytical models in estimating the residual lateral load-carrying capacity of corroded RC columns. A dataset containing 157 rectangular corroded RC columns was analyzed using various design guidelines and analytical models, and their performances were evaluated using performance indices. Among all the design guidelines and analytical models, the EM-3 model (GB 50010–2010 design guideline) and the EM-7 model respectively demonstrated superior performance. Moreover, the EM-7 model excelled among all the considered design guidelines and analytical models, revealing significant values for various performance indices.

Keywords

reinforced concrete, corrosion, RC columns, analytical models, design guidelines

1 Introduction

Reinforced concrete (RC) is one of the most widespread construction materials in modern construction due to its higher durability, strength, and adaptability. RC structures are constructed and formed to satisfy varied architectural and technical requirements and resist different environmental and loading conditions. However, RC structures are not invulnerable to deterioration and damage. Chloride-induced and carbonation-induced corrosion in reinforcing steel (RS) have emerged as the major causes of degradation of these RC structures [1].

The corrosion in RS causes a reduction in the diameter and mechanical properties of the steel [2]. Moreover, the corrosion product exerts higher pressure on surrounding concrete, degrading steel to concrete bond, generating cracks, and causing spalling of concrete [3] that affects the mechanical strength of concrete and ultimately impacts the overall load-carrying capacity (LCC) of the RC structures.

Column in the RC structures is the crucial component that takes all the vertical load and lateral seismic load. However, the corrosion in columns affects the seismic strength of RC structures and may cause the failure of the overall structure under seismic events [4]. Several studies have done experimental investigations to evaluate the failure behavior and seismic capabilities of corroded reinforced concrete (CRC) columns. Lee et al. [5] discovered that the degradation in mechanical and physical characteristics of corroded RS and degradation in bond strength between RS and concrete were the main factors affecting the seismic performance of CRC

columns. Rajput et al. [4] reported that the lateral LCC of CRC columns was reduced by 55.5% and 27% compared to the un-corroded columns, corresponding to 15% and 10% corrosion mass loss respectively. Another study by Guo et al. [6] examined the cyclic performance of the CRC pier and concluded that an increase in the corrosion degree of reinforcement reduces the seismic performance of the pier. Several studies have shown that the energy dissipation capacity, cross-section ductility, ultimate displacement, and LCC of the CRC columns under cyclic lateral loading significantly diminish with an increase in the corrosion level [4, 6–8]. The degree of corrosion and axial load ratio (ALR) have a substantial effect on the failure mode and LCC of CRC columns [9–11]. Moreover, the failure mode of CRC columns under cyclic loads might shift from ductile flexural failure to flexural-shear failure or brittle shear failure due to reduced strength, ductility, and load-carrying capacity caused by corrosion [5, 12]. The combined action of corrosion and seismic forces in RC columns makes them more vulnerable and may cause damage to human life as well as the environment [6]. Therefore, it becomes crucial to assess the residual shear capacity (RSC) of CRC columns so that preventive maintenance and strengthening work can be done before the structure collapses.

2 Research significance

Presently numerous design guidelines and analytical models are available to calculate the shear capacity of RC columns. However, there is a difference between the findings of experiments and the results obtained through design guidelines and analytical models. Consequently, a thorough analysis of the various computed models using a large experiment dataset is required. Therefore, the present study evaluated the performance of existing design guidelines and analytical models in estimating the RSC of CRC columns and suggested the most reliable model that can accurately predict the RSC.

3 Working methodology and experimental dataset

The working methodology of the current study is illustrated in Fig. 1, which started with understanding the problem and reviewing existing literature to explore the analytical models and experimental datasets.

The collected dataset underwent data filtration by excluding the column specimens that were uncorroded and tested without axial load. The final dataset was used to predict the RSC of CRC columns through existing design guidelines and analytical models. The performance and efficacy of the design guidelines and the existing models were evaluated
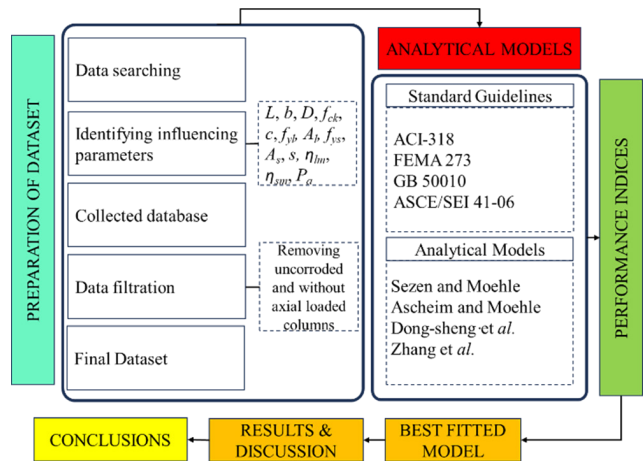

Fig. 1 Working methodology

through the performance indices and the best model was suggested based on the performance results.

3.1 Dataset

Initially, a dataset containing experimental outcomes of RSC of 251 RC columns tested under cyclic lateral load and with or without axial compression load was collected from the published literature. The collected dataset contained both the corroded and uncorroded column specimens. The final data set was then prepared by considering only 157 CRC specimens that were tested under combined axial load and cyclic lateral loading [4–35]. Fig. 2 depicts the configuration of experimental testing of columns, that was adopted by most of the researchers in the literature.
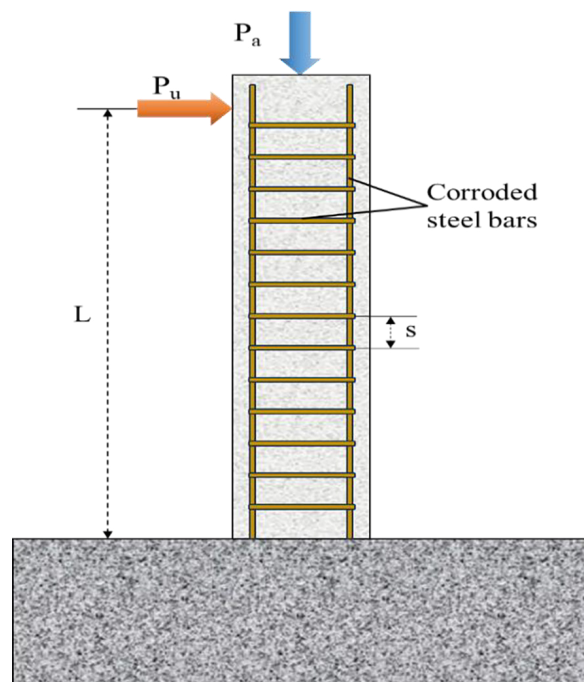

Fig. 2 Testing configuration of column

Table 1 represents the statistical properties such as range, standard deviation (SD), mean, minimum, and maximum values of input parameters such as length of column (L), width of column (b), shear span to depth ratio (λ), depth of column (D), compressive strength of concrete (f_{ck}), clear cover (c), yield strength of longitudinal reinforcement (f_{yl}), area of longitudinal reinforcement (A_l), yield strength of transverse reinforcement (f_{ys}), area of transverse reinforcement (A_s), spacing between transverse reinforcement (s), mass loss of longitudinal reinforcement (η_{lm}), mass loss of transverse reinforcement (η_{sm}), and axial compression load (P_a) to predict the RSC (P_u), which represents the output parameter. It is important to note that the L is the length of the column from the foundation stub's top face to the point of application of lateral load as illustrated in Fig. 2.

3.2 Evaluation criteria

The performance indices like correlation coefficient (R), mean absolute percentage error (MAPE), a20-index, root mean square error (RMSE), Nash–Sutcliffe efficiency index (NS), and mean absolute error (MAE) were used to evaluate the accuracy and performance of the design guidelines and analytical models in predicting the RSC of CRC columns. The values of a20-index, R, and NS closer to 1 indicate the robust positive relationship between the predicted values and experimental values, whereas the values of RMSE, MAPE, and MAE closer to zero indicate the better performance of the model with the least errors [36]. The mathematical expressions of these performance indices are expressed in Eq. (1) to Eq. (6).

$$R = \frac{\sum_{i=1}^{N}\left(X_i - \bar{X}\right)\left(P_i - \bar{P}\right)}{\sqrt{\sum_{i=1}^{N}\left(X_i - \bar{X}\right)^2 \sum_{i=1}^{N}\left(P_i - \bar{P}\right)^2}}, \tag{1}$$

$$\text{MAPE} = \frac{1}{N}\sum_{i=1}^{N}\left|\frac{X_i - P_i}{X_i}\right| \times 100, \tag{2}$$

$$\text{MAE} = \frac{1}{N}\sum_{i=1}^{N}\left|X_i - P_i\right|, \tag{3}$$

$$\text{RMSE} = \sqrt{\frac{\sum_{i=1}^{N}\left(X_i - P_i\right)^2}{N}}, \tag{4}$$

$$\text{NS} = 1 - \frac{\sum_{i=1}^{N}\left(X_i - P_i\right)^2}{\sum_{i=1}^{N}\left(X_i - \bar{P}\right)^2}, \tag{5}$$

$$a20 - \text{index} = \frac{m20}{N}, \tag{6}$$

where N represents the total number of experimental datasets collected, $m20$ is the total number of values derived from X/P values that fall between 0.8 and 1.2, P_i and $\bar{P}$ represent the predicted value and mean of all the predicted values respectively, X_i and $\bar{X}$ represent the experimental value and mean of all the experimental values respectively.

4 Shear capacity estimation
4.1 Design guidelines and analytical models

The RSC of the CRC columns had been predicted using the four design guidelines and four analytical models published in previous studies. Each design guideline and analytical model had given distinct model identity

Table 1 Statistical properties of input and output parameters

Parameters	Symbol	Unit	Minimum	Maximum	Range	Mean	SD
Length of column	L	mm	455.00	2300.00	1845.00	1218.54	433.04
Shear span-to-depth ratio	λ	-	1.75	11.00	9.25	4.16	1.60
Width of column	b	mm	200.00	600.00	400.00	279.87	74.20
Depth of column	D	mm	200.00	400.00	200.00	276.37	57.86
Compressive strength of concrete	f_{ck}	N/mm^2	11.84	56.25	44.41	36.20	11.78
Clear cover	c	mm	10.00	35.00	25.00	25.04	6.97
Yield strength of longitudinal reinforcement	f_{yl}	N/mm^2	298.00	610.00	312.00	448.70	73.38
Area of longitudinal reinforcement	A_l	mm^2	615.75	3926.99	3311.24	1514.54	663.58
Yield strength of transverse reinforcement	f_{ys}	N/mm^2	235.00	607.40	372.40	390.14	91.91
Area of transverse reinforcement	A_s	mm^2	56.55	268.15	211.60	110.61	42.57
Spacing between transverse reinforcement	s	mm	50.00	300.00	250.00	109.14	49.36
Mass loss of longitudinal reinforcement	η_{lm}	%	0.00	67.17	67.17	8.12	8.32
Mass loss of transverse reinforcement	η_{sm}	%	0.00	64.47	64.47	10.54	11.24
Axial compression load	P_a	kN	120.00	1417.60	1297.60	567.07	381.12
Lateral load	P_u	kN	22.63	513.20	490.58	121.06	109.23

to aid clarity such as ACI 318–14 [37], FEMA 273 [38], GB 50010–2010 [39], ASCE/SEI 41–06 [40], Sezen and Moehle [41], Aschheim and Moehle [42], Wang et al. [43], and Zhang et al. [44] were named as EM-1, EM-2, EM-3, EM-4, EM-4, EM-5, EM-6, and EM-7 respectively.

The analytical model proposed by Sezen and Moehle [41], was also used in the ASCE/SEI 41–06 [40]. Therefore, these models provided the same model identity. Table 2 provides detailed information and mathematical expression of all the design guidelines and analytical models that were considered in this study.

The seismic performance in RC structures greatly depends upon the displacement ductility. The displacement ductility is the ratio of ultimate displacement (Δ_u) to the yield point displacement (Δ_y) of the specimen [7, 15, 32] as shown in Fig. 3.

Please note that in the above models, the degraded properties of steel reinforcement were utilized to introduce the effect of corrosion while predicting the RSC of CRC columns. The yield strength (f_{ysc}) and cross-sectional area

(A_{sc}) of corroded stirrups were calculated using the equation proposed by Du et al. [45].

$$f_{ysc} = \left(1 - 0.005\eta_m\right) f_{ys}, \tag{7}$$

$$A_{sc} = \left(1 - 0.01\eta_m\right) A_s, \tag{8}$$

where η_m is the percentage corrosion mass loss of stirrups, f_{ys} and A_s are the yield strength and area of stirrups before corrosion, respectively.

5 Results and discussions

This section presents and describes the predicted outcomes through existing design guidelines and analytical models. The predetermined performance indicators discussed in Section 2.2 and the coefficient of variation (CoV) value, which was derived from the ratio of predicted values to experimental values, were used to compare the outcomes and performance results of the models. It is significant to remember that a CoV value that is closer to zero denotes better predicting outcomes and a smaller deviation from

Table 2 Design guidelines and analytical models

Model	References	Formulation	Remarks
EM-1	ACI 318–14 [37]	$V_n = 0.17\left(1 + \dfrac{N}{13.8A_g}\right)\sqrt{f_c'}\,bd + \dfrac{A_{st}f_{ys}d}{s}$	
EM-2	FEMA 273 [38]	$V_n = 0.29\lambda_o\left(k + \dfrac{N}{13.8A_g}\right)\sqrt{f_c'}\,bd + \dfrac{A_{st}f_{ys}d}{s}$	$k = 1$ (for low ductility demand) $k = 0$ (for moderate to high ductility demand) λ_o is a coefficient depending on concrete weigh
EM-3	GB 50010–2010 [39]	$V_n = \dfrac{1.75}{L_s/d + 1} f_t bd + \dfrac{A_{st}f_{ys}d}{s} + 0.07N$	$f_t = 0.292\sqrt{f_c'}$
EM-4	ASCE/SEI 41–06 [40]; Sezen and Moehle [41]	$V_n = k\left(\dfrac{0.5\sqrt{f_c'}}{L_s/d}\sqrt{1 + \dfrac{N}{0.5\sqrt{f_c'}A_g}}\,0.8A_g + \dfrac{A_{st}f_{ys}d}{s}\right)$	$k = 1$ for $\mu\langle 2; k = 0.7$ for $\mu\rangle 6$; $0.7 \leq k = 1.15 - 0.075\mu \leq 1$ for $2 \leq \mu \leq 6$
EM-5	Aschheim and Moehle [42]	$V_n = 0.3\left(k + \dfrac{N}{13.8A_g}\right)\sqrt{f_c'}\,0.8A_g + \dfrac{A_{st}f_{ys}d}{s\tan\left(30°\right)}$	$k = \dfrac{4-\mu}{3},\ 0 \leq k \leq 1$
EM-6	Wang et al. [43]	$V_n = 0.15C_1 C_2 f_c'\left(0.8A_g\right) + \dfrac{A_{st}f_{ys}d}{s}$	$C_1 = 2.2n + 1,\ C_2 = \dfrac{\alpha}{\mu+2}$ $\alpha = \begin{cases} 3.75/\sqrt{f_c'}, & \mu \leq 2 \\ 3.75/\sqrt{f_c'} - \left(1.46/\sqrt{f_c'}\right)\left(\mu - 2\right), & 2 < \mu < 4 \\ 0.83/\sqrt{f_c'}, & \mu \geq 4 \end{cases}$
EM-7	Zhang et al. [44]	$V_n = \dfrac{1.2k + 24n}{\left(\lambda + 1\right)^3}\sqrt{f_c'}\,bd + \dfrac{A_{st}f_{ys}d}{s}$	$k = 6 - \mu,\ 0 \leq k \leq 1$ $\mu = \dfrac{\left(11\beta_v^{0.5} + 0.6\right)\left(\lambda - 0.5\right)^{0.65-0.9n}}{\left(n + 0.5\right)^2},\ n = \dfrac{N}{A_g f_c}$

V_n is the shear capacity of column, N is the axial compression load, n is ALR, A_g is the gross area of column, b is the width of column, f_c' is the compressive strength of concrete cube, f_c is the compressive strength of concrete cylinder, d is the effective depth of column, A_{st} is the cross-section area of stirrups, f_{ys} is the yield strength of stirrups, s is the center to center spacing between stirrups, L_s is the shear span, μ is the displacement ductility, f_t is the tensile strength of concrete, λ is the shear span to depth ratio, β_v is the stirrups volumetric ratio.
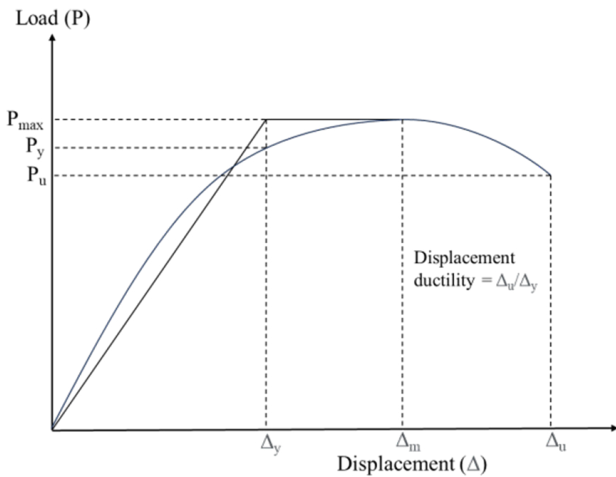
Fig. 3 Displacement ductility of specimen

and performance ratio plots representing the relationship between predicted and experimental values. Additionally, Fig. 4–6 provide a summary of the dataset's distribution across various error and performance ratio ranges, along with mean, SD, CoV values, and performance indices for all design guidelines and analytical models.

5.1 Results of design guidelines

Fig. 4–6 demonstrate that among all design guidelines, the EM-3 model demonstrated the best performance, with impressive values of R (0.7730), a20-index (0.3057), NS (0.6266), MAE (49.38 kN), RMSE (67.83 kN), MAPE (67.02%), and CoV (0.5346). Notably, the EM-3 model exhibited the highest NS and a20-index values, while achieving the lowest values for MAE, RMSE, and MAPE. The EM-4 had the highest R-value of 0.8754, indicating a strong correlation between predicted and experimental values. In contrast, the EM-10 model exhibited the lowest R-value of
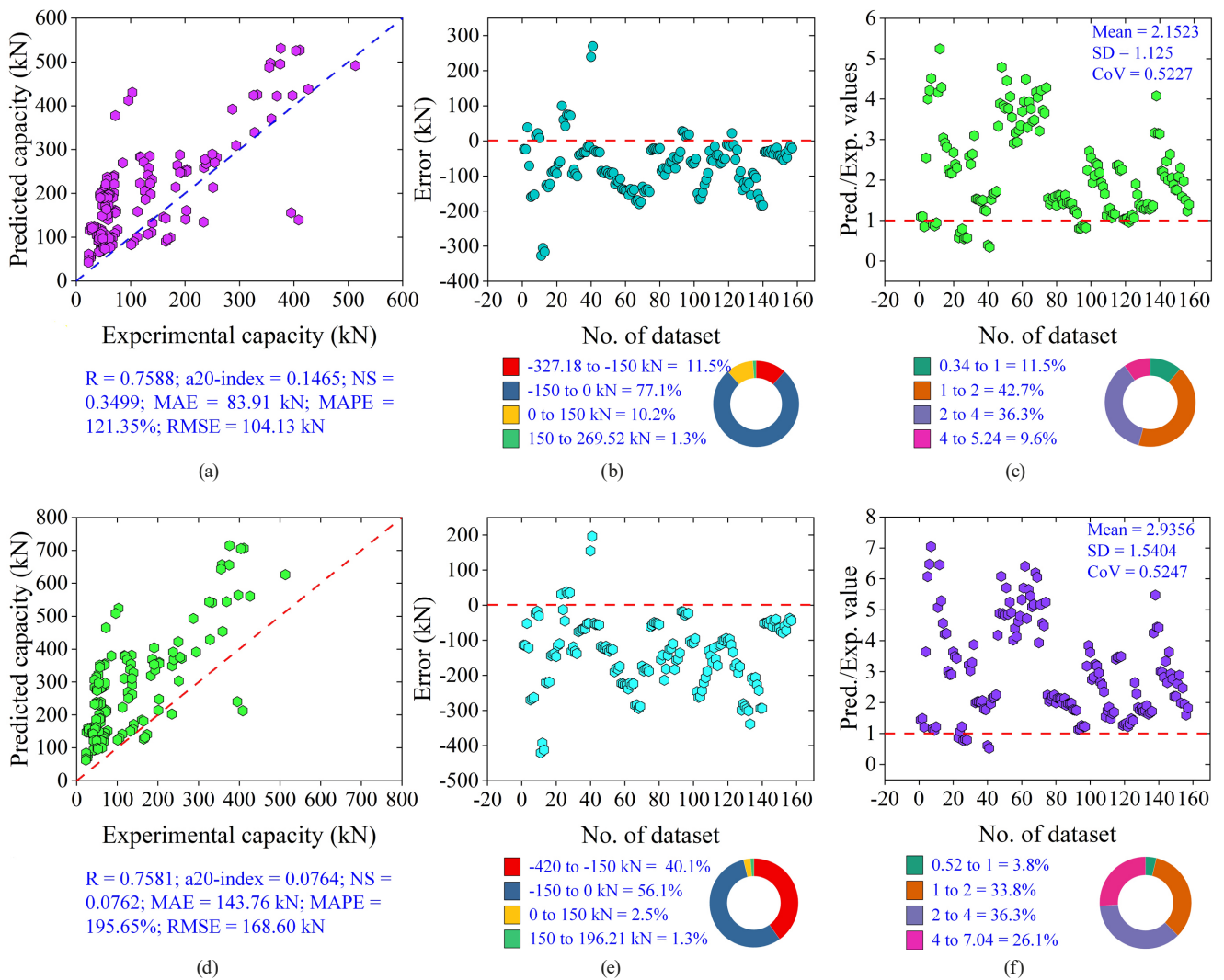
the actual values. Fig. 4–6 illustrate a scatter plot comparing predicted capacity to experimental capacity, as well as error (experimental values – predicted values)

R = 0.7588; a20-index = 0.1465; NS = 0.3499; MAE = 83.91 kN; MAPE = 121.35%; RMSE = 104.13 kN

(a)

-327.18 to -150 kN = 11.5%
-150 to 0 kN = 77.1%
0 to 150 kN = 10.2%
150 to 269.52 kN = 1.3%

(b)

Mean = 2.1523
SD = 1.125
CoV = 0.5227

0.34 to 1 = 11.5%
1 to 2 = 42.7%
2 to 4 = 36.3%
4 to 5.24 = 9.6%

(c)

R = 0.7581; a20-index = 0.0764; NS = 0.0762; MAE = 143.76 kN; MAPE = 195.65%; RMSE = 168.60 kN

(d)

-420 to -150 kN = 40.1%
-150 to 0 kN = 56.1%
0 to 150 kN = 2.5%
150 to 196.21 kN = 1.3%

(e)

Mean = 2.9356
SD = 1.5404
CoV = 0.5247

0.52 to 1 = 3.8%
1 to 2 = 33.8%
2 to 4 = 36.3%
4 to 7.04 = 26.1%

(f)

Fig. 4 Performance of analytical models and design guidelines (a), (d), scatter plot with performance indices, (b), (e), (h) error plot and, (c), (f), (i) performance ratio plot (predicted/experimental values), Fig. 4 (a, b, c) EM-1, Fig. 4 (d, e, f) EM-2
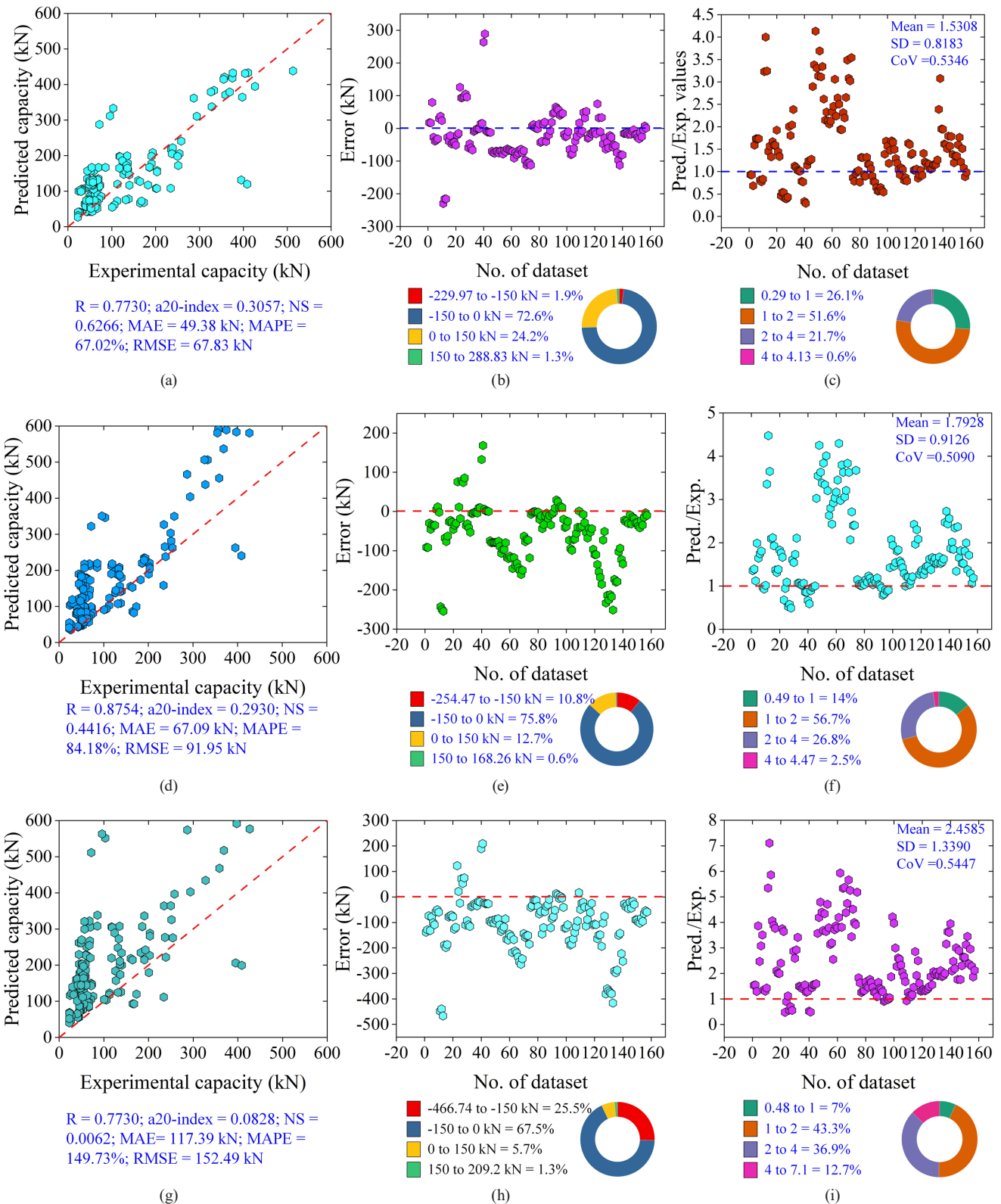
Fig. 5 Performance of analytical models and design guidelines (a), (d), (g) scatter plot with performance indices, (b), (e), (h) error plot and, (c), (f), (i) performance ratio plot (predicted/experimental values), Fig. 5 (a, b, c) EM-3, Fig. 5 (d, e, f) EM-4, Fig. 5 (g, h, i) EM-5

0.7581, suggesting a significantly inferior predictive capability. It's worth noting that the EM-3 model had an *R*-value of 11.69% lower and a CoV value of 5.01% higher than the EM-4 model. Furthermore, when compared to the EM-2 model, which demonstrated the poorest overall performance, the EM-3 model showed significant improvements. Specifically,
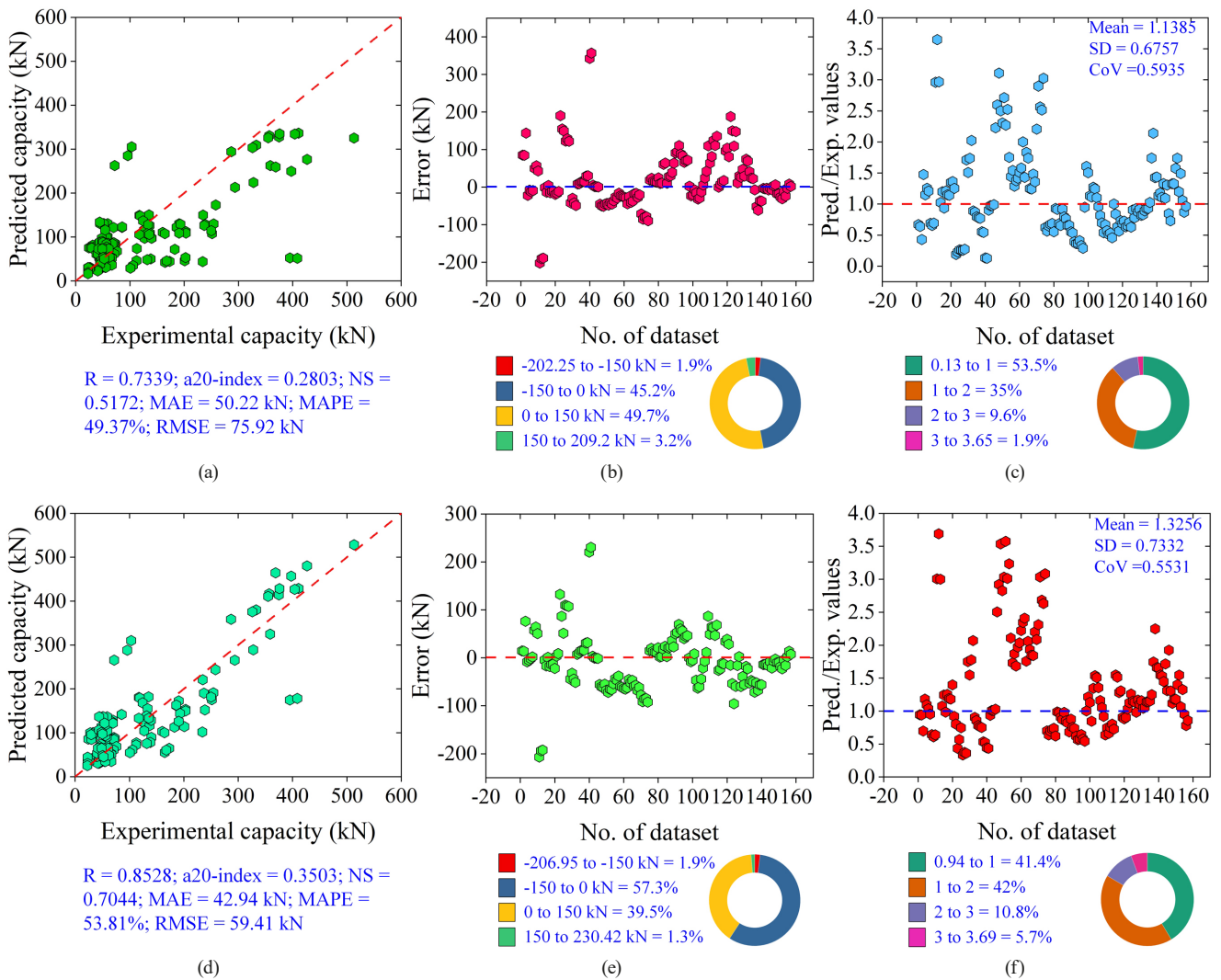
Fig. 6 Performance of analytical models and design guidelines (a), (d), scatter plot with performance indices, (b), (e), (h) error plot and, (c), (f), (i) performance ratio plot (predicted/experimental values), Fig. 6 (a, b, c) EM-6, Fig. 6 (d, e, f) EM-7

the EM-3 model had 1.97%, 300.13%, and 722.31% higher R, a20-index, and NS values respectively. Additionally, it showcased 65.65%, 59.77%, and 65.74% lower MAE, RMSE, and MAPE compared to the EM-2 model.

5.2 Results of analytical models

Fig. 4–6 indicate that among all analytical models, the EM-7 model demonstrated the best overall performance, exhibiting significant values for R (0.8528), a20-index (0.3503), NS (0.7044), MAE (42.94 kN), RMSE (59.41 kN), MAPE (53.81%), and CoV (0.5531). Notably, the EM-7 model exhibited the highest a20-index and NS values, indicating superior efficiency in capturing variability, along with the lowest RMSE and MAE values, suggesting fewer prediction errors. However, it had a 2.58% lower R-value, 9% higher MAPE value, and 8.66% higher CoV than EM-4, EM-6, and EM-4 models respectively.

Fig. 4–6 also highlight that the EM-4 model had the lowest CoV value of 0.5090 and the highest R-value of 0.8754, indicating strong alignment between estimated and experimental values with minimal deviations. Conversely, the EM-6 model showed the highest CoV value of 0.5935 and the lowest R-value of 0.7339, suggesting a notably inferior predictive capability.

Furthermore, the EM-5 model demonstrated the lowest performance results with poor values of R (0.7730), a20-index (0.0828), NS (0.0062), MAE (117.39 kN), RMSE (152.49 kN), MAPE (149.73%), and CoV (0.5447). Compared to the EM-5 model, the EM-7 model exhibited 10.32%, 323.07%, and 11261.29% higher R, a20-index, and NS values respectively. Additionally, it had 63.42%, 61.04%, 64.06%, and 1.54% lower MAE, RMSE, MAPE, and CoV values respectively.

5.3 Discussions

Among the design guidelines and analytical models, the EM-3 and EM-7 exhibited the best overall performance, respectively. Upon comparing these two models, it becomes evident that the EM-7 model surpassed the EM-3 model. It demonstrated 14.59%, 10.31%, and 12.42% higher values for a20-index, R, and NS, while also showing 13.04%, 12.41%, and 19.71% lower values for MAE, RMSE, and MAPE, respectively. However, it's important to note that the EM-7 model had a slightly higher CoV value (0.5531) compared to the EM-3 model (0.5346). Despite this small difference, it can be concluded that the EM-7 model outperformed all design guidelines and analytical models based on the overall performance results.

In the performance ratio plot of Fig. 4–6, when the Pred./Exp. values are 1, which means that the predicted values match the actual values exactly. Likewise, if the values are less than 1, it suggests that the results are underestimated, whereas values exceeding 1 imply overestimation Additionally, in the error plot of Fig. 4–6, an error of zero indicate perfect alignment between predicted and actual values. Positive errors suggest underestimation, whereas negative errors imply overestimation. Notably, Fig. 4–6 reveal that the EM-2 model exhibit the highest percentage of the dataset (96.2%) with negative errors and the lowest percentage of the dataset (3.8%) with Pred./Exp. value less than one, indicating overestimated results. Conversely, the EM-6 model demonstrates the lowest percentage of dataset (47.1%) with negative errors and the highest percentage of a dataset (53.5%) with Pred./Exp. value less than one.

Furthermore, the output of all the design guidelines and analytical models demonstrated that the seismic strength of CRC columns decreased significantly with increasing the axial load ratio and degree of corrosion. This observed phenomenon is consistent with prior investigations [16, 23, 33], which have similarly underscored the adverse impact of these factors on seismic strength.

6 Conclusions

This study presented and evaluated four design guidelines and four analytical models for the residual shear capacity prediction of corroded RC columns subjected to both axial load and cyclic lateral loading. A dataset comprising 157 experimental rectangular corroded RC column specimens was utilized to assess and compare the reliability and performance of these models based on performance indices (R, a20-index, NS, RMSE, MAPE, MAE, and CoV).

The following conclusions were drawn:

- Among all the design guidelines evaluated, the EM-3 model (GB 50010-2010 [39] design guideline) demonstrated the best performance, with notable values of R (0.7730), a20-index (0.3057), NS (0.6266), MAE (49.38 kN), RMSE (67.83 kN), MAPE (67.02%), and CoV (0.5346).
- In terms of analytical models, the EM-7 model [44] exhibited superior overall performance, with significant values of R, NS, a20-index, RMSE, MAE, MAPE, and CoV being 0.8528, 0.7044, 0.3503, 59.41 kN, 42.94 kN, 53.81%, and 0.5531, respectively.
- Compared to the best design guideline (EM-3 model), the best analytical model (EM-7 model) displayed R, NS, and a20-index values that were 10.31%, 12.42%, and 14.59% higher, respectively.
- The EM-7 model also showed lower MAE, RMSE, and MAPE values by 13.04%, 12.41%, and 19.71%, respectively, compared to the EM-3 model.
- Overall, among all considered analytical models and design guidelines, the EM-7 model exhibited the best performance, followed by EM-3, EM-4, EM-6, EM-1, EM-5, and EM-2 models in descending order of effectiveness.
- The EM-7 model showed a slightly (2.58%) lower R-value and higher (8.66%) CoV value than the EM-4 model.
- The EM-2 model showed the highest percentage of dataset (96.2%) with a negative error value, indicating overestimated predicted results.

This study concluded that, among all the evaluated design guidelines and analytical models in predicting the residual shear capacity of corroded RC columns, the EM-3 (GB 50010–2010 [39] design guideline) model and EM-7 model [44] exhibited the best performances, respectively. The superior performance of the EM-3 and EM-7 models highlights the potential for practical application in structural assessment and retrofitting strategies. Furthermore, this study provides valuable insights for researchers and structural engineers in selecting the most effective model for predicting the RSC of CRC columns.

6.1 Limitations

The study predominantly considered only rectangular CRC columns, neglecting the different column geometries (circular) in the dataset. Additionally, the limited number

of specimens in the dataset may not fully capture the accuracy and reliability of the design guidelines and analytical models in predicting the RSC of CRC columns.

6.2 A way forward

In future studies, it would be beneficial to include a broader range of column shapes, sizes, and configurations in the dataset. This expanded dataset would better represent the diversity encountered in real-world applications, providing a more comprehensive foundation for developing and validating models. The results obtained through the available design guidelines and analytical models, it evident that these analytical models and design guidelines do not provide significant results, because the available design guidelines and analytical models do not consider all the responsible factors that affect the residual capacity of corroded columns. Therefore, there is a need for the development of a more reliable and accurate analytical or machine learning-based model in the future, capable of precisely predicting the RSC of CRC columns.

References

[1] Ahmed E S, J., Ganesh, G. M. "A comprehensive overview on corrosion in RCC and its prevention using various green corrosion inhibitors", Buildings, 12(10), 1682, 2022.
https://doi.org/10.3390/buildings12101682

[2] Almusallam, A. A. "Effect of degree of corrosion on the properties of reinforcing steel bars", Construction and Building Materials, 15(8), pp. 361–368, 2001.
https://doi.org/10.1016/S0950-0618(01)00009-5

[3] Yang, Y., Nakamura, H., Miura, T., Yamamoto, Y. "Effect of corrosion-induced crack and corroded rebar shape on bond behavior", Structural Concrete, 20(6), pp. 2171–2182, 2019.
https://doi.org/10.1002/suco.201800313

[4] Rajput, A. S., Sharma, U. K., Engineer, K. "Seismic retrofitting of corroded RC columns using advanced composite materials", Engineering Structures, 181, pp. 35–46, 2019.
https://doi.org/10.1016/j.engstruct.2018.12.009

[5] Lee, H.-S., Kage, T., Noguchi, T., Tomosawa, F. "An experimental study on the retrofitting effects of reinforced concrete columns damaged by rebar corrosion strengthened with carbon fiber sheets", Cement and Concrete Research, 33(4), pp. 563–570, 2003.
https://doi.org/10.1016/S0008-8846(02)01004-9

[6] Guo, A., Li, H., Ba, X., Guan, X., Li, H. "Experimental investigation on the cyclic performance of reinforced concrete piers with chloride-induced corrosion in marine environment", Engineering Structures, 105, pp. 1–11, 2015.
https://doi.org/10.1016/j.engstruct.2015.09.031

[7] Yang, S.-Y., Song, X.-B., Jia, H.-X., Chen, X., Liu, X.-L. "Experimental research on hysteretic behaviors of corroded reinforced concrete columns with different maximum amounts of corrosion of rebar", Construction and Building Materials, 121, pp. 319–327, 2016.
https://doi.org/10.1016/j.conbuildmat.2016.06.002

[8] Li, Q., Niu, D., Xiao, Q., Guan, X., Chen, S. "Experimental study on seismic behaviors of concrete columns confined by corroded stirrups and lateral strength prediction", Construction and Building Materials, 162, pp. 704–713, 2018.
https://doi.org/10.1016/j.conbuildmat.2017.09.030

[9] Dai, K.-Y., Lu, D-G., Yu, X.-H. "Experimental investigation on the seismic performance of corroded reinforced concrete columns designed with low and high axial load ratios", Journal of Building Engineering, 44, 102615, 2021.
https://doi.org/10.1016/j.jobe.2021.102615

[10] Vu, N. S., Li, B. "Seismic performance of flexural reinforced concrete columns with corroded reinforcement", ACI Structural Journal, 115(5), pp. 1253–1266, 2018.
https://doi.org/10.14359/51702372

[11] Vu, N. S., Li, B. "Seismic performance assessment of corroded reinforced concrete short columns", Journal of Structural Engineering, 144(4), 04018018, 2018.
https://doi.org/10.1061/(ASCE)ST.1943-541X.0001994

[12] Meda, A., Mostosi, S., Rinaldi, Z., Riva, P. "Experimental evaluation of the corrosion influence on the cyclic behaviour of RC columns", Engineering Structures, 76, pp. 112–123, 2014.
https://doi.org/10.1016/j.engstruct.2014.06.043

[13] Rinaldi, Z., Di Carlo, F., Spagnuolo, S., Meda, A. "Influence of localised corrosion on the cyclic response of reinforced concrete columns", Engineering Structures, 256, 114037, 2022.
https://doi.org/10.1016/j.engstruct.2022.114037

[14] Ma, G., Li, H., Hwang, H.-J. "Seismic behavior of low-corroded reinforced concrete short columns in an over 20-year building structure", Soil Dynamics and Earthquake Engineering, 106, pp. 90–100, 2018.
https://doi.org/10.1016/j.soildyn.2017.12.006

[15] Shang, Z., Zheng, S., Zheng, H., Li, Y., Dong, J. "Seismic behavior and damage evolution of corroded RC columns designed for bending failure in an artificial climate", Structures, 38, pp. 184–201, 2022.
https://doi.org/10.1016/j.istruc.2022.01.072

[16] Yalciner, H., Kumbasaroglu, A. "Experimental evaluation and modeling of corroded reinforced concrete columns", ACI Structural Journal, 117(4), pp. 61–76, 2020.
https://doi.org/10.14359/51721372

[17] Dai, K.-Y., Liu, C., Lu, D-G., Yu, X.-H. "Experimental investigation on seismic behavior of corroded RC columns under artificial climate environment and electrochemical chloride extraction: A comparative study", Construction and Building Materials, 242, 118014, 2020.
https://doi.org/10.1016/j.conbuildmat.2020.118014

[18] Zheng, H., Zheng, S., Zhang, Y., Cai, Y., Ming, M., Zhou, J. "Experimental investigation on seismic behaviours of reinforced concrete columns under simulated acid rain environment", Advances in Civil Engineering, 2020(1), 3826062, 2020.
https://doi.org/10.1155/2020/3826062

[19] Li, X., Zhao, Z.-H., Liang, Y.-S., Lv, H.-L. "Cyclic behaviour of earthquake- and corrosion-damaged RC columns", Magazine of Concrete Research, 68(22), pp. 1166–1182, 2016.
https://doi.org/10.1680/jmacr.16.00155

[20] Luo, X., Cheng, J., Xiang, P., Long, H. "Seismic behavior of corroded reinforced concrete column joints under low-cyclic repeated loading", Archives of Civil and Mechanical Engineering, 20(2), 40, 2020.
https://doi.org/10.1007/s43452-020-00043-z

[21] Celik, A., Yalciner, H., Kumbasaroglu, A., Turan, A. İ. "An experimental study on seismic performance levels of highly corroded reinforced concrete columns", Structural Concrete, 23(1), pp. 32–50, 2022.
https://doi.org/10.1002/suco.202100065

[22] Zhang, D., Zhao, Y., Jin, W., Ueda, T., Nakai, H. "Shear strengthening of corroded reinforced concrete columns using pet fiber based composties", Engineering Structures, 153, pp. 757–765, 2017.
https://doi.org/10.1016/j.engstruct.2017.09.030

[23] Rajput, A. S., Sharma, U. K. "Corroded reinforced concrete columns under simulated seismic loading", Engineering Structures, 171, pp. 453–463, 2018.
https://doi.org/10.1016/j.engstruct.2018.05.097

[24] Karimipour, A., Edalati, M. "Retrofitting of the corroded reinforced concrete columns with CFRP and GFRP fabrics under different corrosion levels", Engineering Structures, 228, 111523, 2021.
https://doi.org/10.1016/j.engstruct.2020.111523

[25] Rajput, A. S., Sharma, U. K. "Performance of aged reinforced concrete columns under simulated seismic loading", Structural Concrete, 20(3), pp. 1123–1136, 2019.
https://doi.org/10.1002/suco.201800235

[26] Li, J., Gong, J., Wang, L. "Seismic behavior of corrosion-damaged reinforced concrete columns strengthened using combined carbon fiber-reinforced polymer and steel jacket", Construction and Building Materials, 23(7), pp. 2653–2663, 2009.
https://doi.org/10.1016/j.conbuildmat.2009.01.003

[27] Xu, Y.-Y., Huang, J.-Q. "Cyclic performance of corroded reinforced concrete short columns strengthened using carbon fiber-reinforced polymer", Construction and Building Materials, 247, 118548, 2020.
https://doi.org/10.1016/j.conbuildmat.2020.118548

[28] Chang, Z. Q., Xing, G. H., Luo, D. M., Liu, B. Q. "Seismic behaviour and strength prediction of corroded RC columns subjected to cyclic loading", Magazine of Concrete Research, 72(17), pp. 900–918, 2020.
https://doi.org/10.1680/jmacr.18.00181

[29] Goksu, C., Ilki, A. "Seismic behavior of reinforced concrete columns with corroded deformed reinforcing bars", ACI Structural Journal, 113(5), 2016.
https://doi.org/10.14359/51689030

[30] Yin, S., Yang, Y., Ye, T., Li, Y. "Experimental research on seismic behavior of reinforced concrete columns strengthened with TRC under corrosion environment", Journal of Structural Engineering, 143(5), 04016231, 2017.
https://doi.org/10.1061/(ASCE)ST.1943-541X.0001713

[31] Funaki, H., Yamakawa, T., Nakada, K. "Experimental studies on durability and seismic performance of real-scaled RC columns exposed at a coastal area in Okinawa", Journal of Structural and Construction Engineering (Transactions of the AI J), 76(666), pp. 1479–1488, 2011. (in Japanese)
https://doi.org/10.3130/aijs.76.1479

[32] Li, D., Wei, R., Xing, F., Sui, L., Zhou, Y., Wang, W. "Influence of non-uniform corrosion of steel bars on the seismic behavior of reinforced concrete columns", Construction and Building Materials, 167, pp. 20–32, 2018.
https://doi.org/10.1016/j.conbuildmat.2018.01.149

[33] Zhang, W., Liu, Y., Hu, F., Gu, X. "Experimental and numerical investigation on seismic performance of corroded RC columns of low-strength concrete", Bulletin of Earthquake Engineering, 21(4), pp. 2103–2140, 2023.
https://doi.org/10.1007/s10518-022-01593-8

[34] Shi, Q. X., Niu, D. T., Yan, G. Y. "Experimental research on hysteretic characteristics of corroded RC members with flexural and compressive axial loads under repeated horizontal loading", Earthquake Engineering and Engineering Vibration, 20(4), pp. 44–50, 2000. (in Chinese)
https://doi.org/10.13197/j.eeev.2000.04.007

[35] Zheng, S. S., Dong, L. G., Zuo, H. S., Qin, Q., Liu, W., Li, Q. Q. "Experimental investigation on seismic behaviors of corroded RC frame columns in artificial climate", Journal Building Structures, 39(4), pp. 28–36, 2018. (in Chinese)
https://doi.org/10.14006/j.jzjgxb.2018.04.004

[36] Kumar, A., Arora, H. C., Kapoor, N. R., Kumar, K., Hadzima-Nyarko, M., Radu, D. "Machine learning intelligence to assess the shear capacity of corroded reinforced concrete beams", Scientific Reports, 13(1), 2857, 2023.
https://doi.org/10.1038/s41598-023-30037-9

[37] ACI "ACI 318-14 Building code requirements for structural concrete", American Concrete Institute, Farmington Hills, MI, USA, 2014.

[38] FEMA " NEHRP guidelines for the Seismic Rehabilitation of Buildings", Federal Emergency Management Agency, Washington, DC, USA, FEMA 273, 1997.

[39] Ministry of Housing and Urban-Rural Development of the People's Republic of China "GB 50010-2010 Code for design of concrete structures", Standardization Administration of China, Beijing, China, 2010.

[40] ASCE "ASCE/SEI-41-06 Seismic rehabilitation of existing buildings", Seismic Rehabilitation Standards Committee, American Society of Civil Engineers, Reston, VA, USA, 2007.
https://doi.org/10.1061/9780784408841

[41] Sezen, H., Moehle, J. P. "Shear strength model for lightly reinforced concrete columns", Journal of Structural Engineering, 130(11), pp. 1692–1703, 2004.
https://doi.org/10.1061/(ASCE)0733-9445(2004)130:11(1692)

[42] Aschheim, M., Moehle, J. P. "Shear strength and deformability of RC bridge columns subjected to inelastic cyclic displacements", University of California at Berkeley, Berkeley, CA, USA, Rep. UCB/EERC-92/04, 1992. [online] Available at: https://ntrl.ntis.gov/NTRL/dashboard/searchResults/titleDetail/PB93120327.xhtml/

[43] Wang, D., Si, B., Sun, Z., Li, X., Ai, Q. "Experiment on shear strength of reinforced concrete bridge column in plastic hinge zone under seismic effect", China Journal of Highway and Transport, 24(2), pp. 34–41, 2011. [online] Available at: https://www.researchgate.net/publication/290537092_Experiment_on_shear_strength_of_reinforced_concrete_bridge_column_in_plastic_hinge_zone_under_seismic_effect (in Chinese)

[44] Zhang, Q., Gong, J., Ma, Y. "Seismic shear strength and deformation of RC columns failed in flexural shear", Magazine of Concrete Research, 66(5), pp. 234–248, 2014.
https://doi.org/10.1680/macr.13.00221

[45] Du, Y. G., Clark, L. A., Chan, A. H. C. "Residual capacity of corroded reinforcing bars", Magazine of Concrete Research, 57(3), pp. 135–147, 2005.
https://doi.org/10.1680/macr.2005.57.3.135